Mössbauer study of 1% Fe doped $LaMnO_3$ compound

2004 J. Phys.: Condens. Matter 16 7419

(http://iopscience.iop.org/0953-8984/16/41/021)

INSTITUTE OF PHYSICS PUBLISHING JOURNAL OF PHYSICS: CONDENSED MATTER

J. Phys.: Condens. Matter **16** (2004) 7419–7426 PII: S0953-8984(04)84902-6

Mössbauer study of 1% Fe doped $LaMnO_3$ compound

M Pissas and A Simopoulos

Institute of Materials Science, NCSR, Demokritos, 15310 Aghia Paraskevi, Athens, Greece

Received 12 August 2004
Published 1 October 2004
Online at stacks.iop.org/JPhysCM/16/7419
doi:10.1088/0953-8984/16/41/021

Abstract

Using Mössbauer spectroscopy we have studied stoichiometric and cation deficient $LaMnO_3$ compounds. The Mössbauer spectra of the stoichiometric $LaMnO_3$ compound can be interpreted within the cooperative orbital ordered A-antiferromagnetic structure. The cation deficient sample displays spectra which correspond to the orbital 'glass' state without any local signature of Jahn–Teller distorted octahedra.

(Some figures in this article are in colour only in the electronic version)

1. Introduction

Stoichiometric $LaMnO_3$ is an A-type antiferromagnet with ferromagnetic interactions in the a–c-planes and antiferromagnetic interactions along the b-axis between successive ac-layers (see [1] and references therein). The ionic state of Mn is $(t_{2g}^3 e_g^1)$ with total spin $S = 2$. In addition $LaMnO_3$ has an antiferro-orbital ordering with locally elongated octahedra packed so that the long axis alternates in the basal plane (see figure 1) minimizing the total stain energy. This orbital ordering results from the cooperative Jahn–Teller effect taking place as a consequence of the breaking of orbital degeneracy of the E_g state by coupling to phonons. The orbital ordering in the basal (a–c) plane is formed by a short and a long bond resulting in an overlap of nearly half-filled with empty orbitals through 2p oxygen orbitals so that the superexchange interactions are ferromagnetic. Along the b-axis, Mn ions are connected with O(1) so that only one type of bond exists in the Mn–O(1)–Mn path, leading to antiferromagnetic superexchange interactions.

An additional ferromagnetic component along b-axis exists, due to a small antisymmetric Dzialoshinskii–Moriya coupling [2]. Depending on the preparation condition the nominal $LaMnO_3$ compound displays a defect structure [3–7]. If the sample is cooled from high temperature (1400 °C) in air atmosphere then the tendency of Mn for higher oxidation states creates randomly distributed vacancies. These vacancies drastically modify the magnetic properties of the compound. The most important change is the appearance of ferromagnetic long range order. Despite the intense research effort, the basic mechanism which is responsible for this drastic change is not comprehensible enough. In order to elucidate this type of problem

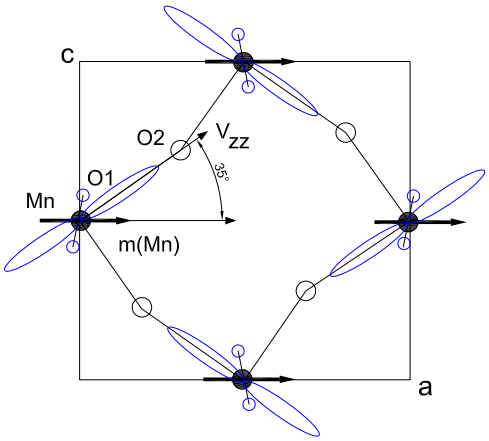

Figure 1. Projection of an Mn–O layer in the ac-plane. The Mn^{3+} magnetic moments are ferromagnetically coupled in the layer and are directed along the a-axis ($Pnma$ notation). The principal axes of the EFG tensor approximately coincide with the axes of the Mn octahedron, with the V_{zz} axis along the long Mn–O bond.

experimental information at the local level is absolutely necessary. Techniques like NMR and Mössbauer spectroscopy can give valuable information concerning the role of the local structure (electronic or magnetic) in the global properties of the $LaMnO_3$ compound. In manganese perovskites Mössbauer spectroscopy in low ^{57}Fe-and ^{119}Sn-doped samples [8–16] has contributed useful information. Mössbauer spectroscopy senses the local environment of probe atoms (^{57}Fe in our case) substituted into Mn sites by observing the magnetic hyperfine field and electric field gradient (EFG) generated by the electrons and nuclei that surround them. In the present study, we use stoichiometric and cation deficient 1% ^{57}Fe-doped $LaMnO_{3+\delta}$ in an attempt to understand at the local level the differences of the two compounds.

2. Experimental details

A sample with nominal composition $LaMn_{0.99}Fe_{0.01}O_3$ was prepared by the standard solid state reaction method using Fe_2O_3 90% enriched with ^{57}Fe. We prepared two samples. The first sample was prepared at 1400 °C in air atmosphere. We call this sample the air prepared sample (AP). The second sample was annealed in the final stage (of the preparation at) 1000 °C in reduced atmosphere, and we call it the reduced sample (R). The x-ray diffraction data show single phase materials. The x-ray diffraction patterns for both samples were analysed using the Rietveld refinement method, assuming the orthorhombic $Pnma$ space group. The AP sample has unit cell parameters ($a = 5.4941(1)$ Å, $b = 7.7789(1)$ Å and $c = 5.5308(1)$ Å), while R displays unit cell parameters ($a = 5.7410(1)$ Å, $b = 7.6873(1)$ Å, and $c = 5.5319(1)$ Å) which correspond to the stoichiometric $LaMnO_3$ sample [17]. The absorption Mössbauer spectra (MS) were recorded using a conventional constant acceleration spectrometer with a ^{57}Co (Rh) source moving at room temperature, while the absorber was kept fixed in a variable temperature cryostat equipped with a 65 kOe superconductive magnet with the field being perpendicular to the γ-rays. The resolution was determined to be $\Gamma/2 = 0.14$ mm s^{-1} using a thin α-Fe foil. DC magnetization measurements were performed in a SQUID magnetometer (Quantum Design). A home-made AC susceptometer was also used.

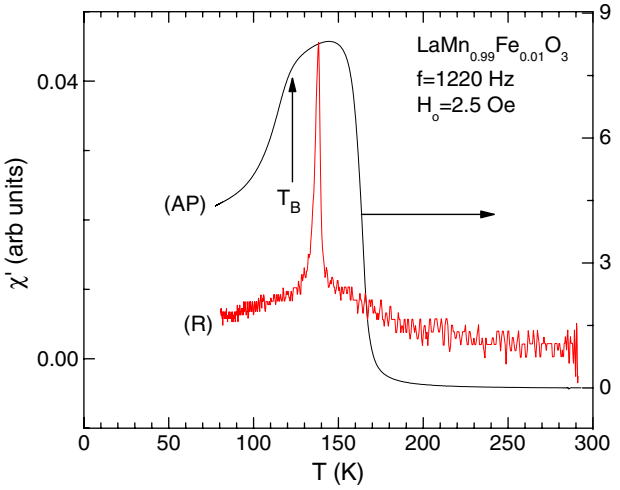

Figure 2. Temperature variation of the AC susceptibility of the R and AP $LaMnO_3$ samples.

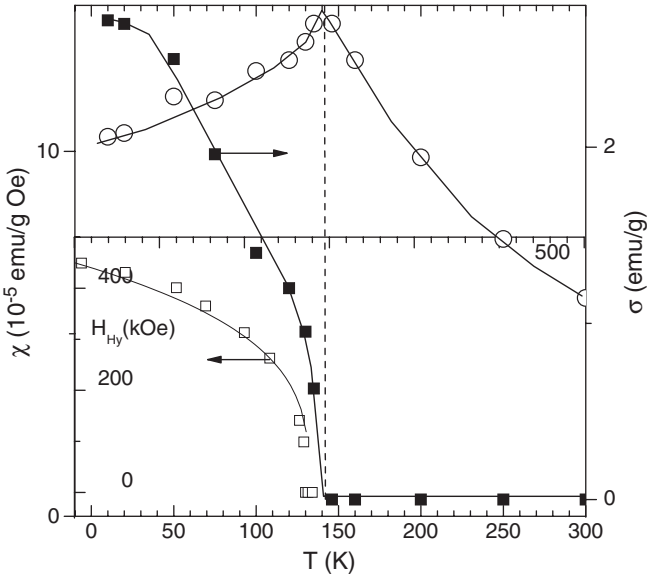

Figure 3. Temperature variation of the magnetic susceptibility $\chi = \mathrm{d}m/\mathrm{d}H$ (for $H > 10$ kOe) (open circles) of the ferromagnetic magnetic moment σ (solid squares) and of the hyperfine magnetic field (open squares). The solid line is a plot of the $H_{\mathrm{hy}} = H_0(1 - T/T_{\mathrm{c}})^{\beta}$, $\beta = 0.3$.

3. Magnetic measurements

Figure 2 shows the temperature variation of the AC susceptibility for the AP and R samples. The overall variation of the χ' of the AP sample is similar to that observed in all the AP $La_{1-x}Ca_xMnO_3$ ($x = 0$–0.2) samples. The sharp rise corresponds to a ferromagnetic transition, while the drop at T_{B} may be related to the orbital rearrangement. On the other hand, the $\chi'(T)$ of the R sample displays a narrow peak at T_{N}. This behaviour is the result of the canted antiferromagnetic structure of the stoichiometric $LaMnO_3$ compound [2].

Figure 3 illustrates the temperature variation of the ferromagnetic component deduced from isothermal measurements (not shown) by extrapolating the high field linear variation to zero field. We have also plotted, in the same figure, the temperature variation of the magnetic susceptibility $\chi = \mathrm{d}m/\mathrm{d}H$ which is estimated from the slope of the linear variation of the $m(H)$-curves. The ferromagnetic component displays a power law variation, resembling

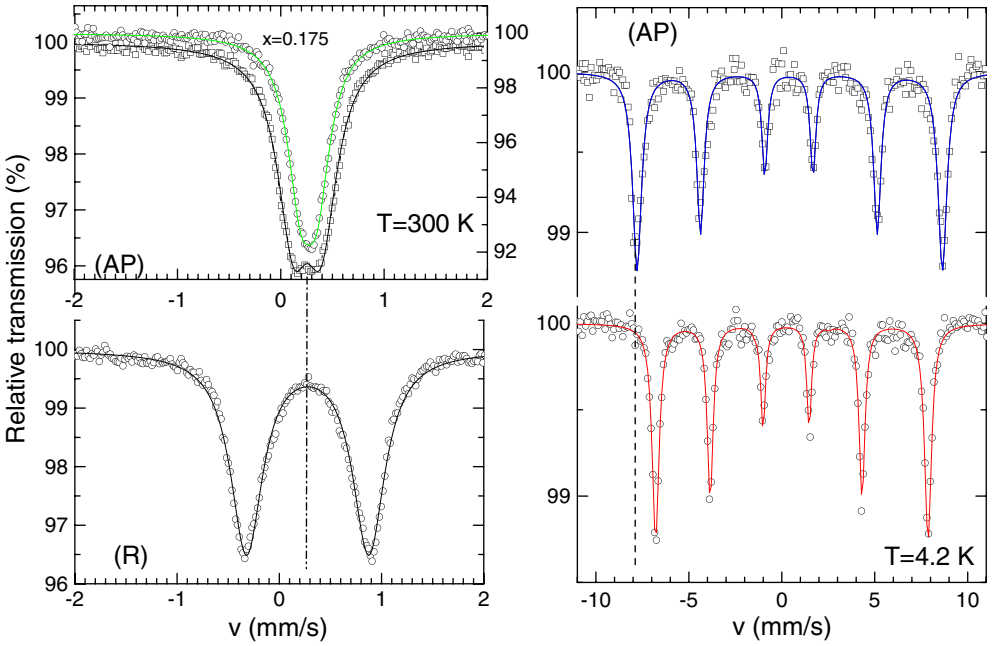

Figure 4. Mössbauer spectra of AP and R $LaMnO_3$ samples at $T = 300$ and 4.2 K. The room temperature spectrum of the $x = 0.175$ sample is also displayed for comparison.

typical ferromagnetic behaviour. On the other hand, χ displays a peak at T_N, as in the case of an antiferromagnet. Such a behaviour has been predicted theoretically in the case of a canted antiferromagnet [18, 19].

4. Mössbauer spectra

Figure 4 shows the MS at $T = 300$ and 4.2 K, for both AP and R samples, in order to clearly show the difference between them. For the AP sample, at $T = 300$ K the MS consists of a nearly unresolved doublet with isomer shift $\delta = 0.379(1)$ mm s^{-1} and quadrupole splitting $\Delta E_Q = (e^2Qq/2)(1+\eta^2/3)^{1/2} = 0.276(1)$ mm s^{-1}, where $Q = 0.213$ cm^2 is the nuclear quadrupole moment of ^{57}Fe, $q = V_{zz}/|e|$, $\eta = (V_{xx} - V_{yy})/V_{zz}$, V_{xx}, V_{yy}, V_{zz} are the components of EFG tensor along its principal axes x, y, z, and $|e|$ is the proton charge. The line width, $\Gamma/2 = 0.18$ mm s^{-1}, is slightly larger than that obtained from the calibration ($\Gamma/2 = 0.14$ mm s^{-1}). The hyperfine parameters for the R sample are $\delta = 0.383(1)$ mm s^{-1}, $\Delta E_Q = 1.094$ mm s^{-1} and $\Gamma/2 = 0.19$ mm s^{-1}. The isomer shift values for both samples are typical for Fe^{3+}. The quantity $(q/2)(1+\eta^2/3)^{1/2}$ for the R sample is significantly larger than for the AP one, a fact which is in agreement with the XRD data. The reduced sample has unit cell parameters that correspond to the characteristic orbital ordered state of the stoichiometric $LaMnO_3$ sample below the Jahn–Teller temperature [1] ($T_{JT} = 750$ K). In this case the Mn ions are coordinated by an oxygen octahedron with four nearly equal bonds and two long bonds (see figure 1). The long bonds are located in a zigzag fashion in the ac-plane, along the [101] and [10$\bar{1}$] directions.

The MS at $T = 4.2$ K show very interesting characteristics. For the AP sample the spectrum consists of a magnetically split sextet with $\delta = 0.511$ mm s^{-1}, $H = 512$ kOe and $\epsilon = (3/2)(3\cos^2\Theta - 1 + \eta\sin^2\Theta\cos 2\Phi)e^2Q/12 = 0.023(4)$ mm s^{-1}. The spectrum of the R sample is also magnetically split but with significantly lower hyperfine magnetic field. In

Table 1. Half linewidth $\Gamma/2$ (mm s^{-1}), isomer shift δ relative to metallic Fe at room temperature (mm s^{-1}), hyperfine magnetic field H (kG), quadrupole parameters QP, $QP_1 = (1/2)|e|V_{zz}Q(1+\eta^2/3)^{1/2}$, $QP_2 = |e|V_{zz}Q$ and $QP_3 = (3/2)(3\cos^2\Theta - 1 + \eta\sin^2\Theta\cos 2\Phi)e^2Q/12$ for the paramagnetic, the magnetic (full diagonalization) and magnetic (first order perturbation theory) cases respectively; Θ and Φ are the polar angles of the hyperfine magnetic field with respect to the principal EFG axes. The estimated hyperfine parameters are obtained from least squares fits of the Mössbauer spectra of the AP and R $LaMn_{0.99}Fe_{0.01}O_3$ samples. The numbers in parentheses are estimated standard deviations referring to the last significant digit. The values at the lines with (*) mean theoretically calculated using the point charge approximation.

	T (K)	δ	QP	$\Gamma/2$	H	ΔH	Θ	Φ	η
AP	300	0.379(2)	$QP_1 = 0.376(1)$	0.187(1)	—	—	—	—	—
AP*	300	—	$QP_1 = 0.081(3)$	—	—	—	—	—	—
R	300	0.383(2)	$QP_1 = 1.094(3)$	0.19(2)	—	—	—	—	—
R*	300	—	$QP_1 = 1.118$	—	—	—	—	—	0.387
AP	4.2	0.511(4)	$QP_3 = 0.023(4)$	0.16	512	7	—	—	—
AP*	4.2	—	—	—	—	—	—	—	—
R	4.2	0.492	$QP_2 = 2.34(3)$	0.14(1)	449(1)	5	40(1)	252(10)	0.45(5)
R*	4.2	—	$QP_2 = 2.20$				34.1	254	0.454

trying to fit this spectrum supposing that the quadrupole interaction is a first order perturbation of the magnetic hyperfine Hamiltonian, we conclude that this is not the case. Consequently, we employed a complete diagonalization of the nuclear Hamiltonian taking into account the equal footing of the magnetic and quadrupole interactions. Despite this complication, we can calculate the direction of the magnetic hyperfine field with respect to the principal axes of the EFG, the asymmetry parameter and V_{zz}.

It is very difficult to fit the MS spectra leaving as free parameters the polar angles (Θ, Φ) of the magnetic hyperfine field with the principal axes of the EFG tensor and the asymmetry parameter η. We estimate these parameters by calculating the electric field gradient at the Mn site using the available crystal structure data of Moussa *et al* [1]. Using the point charge approximation we calculated the EFG tensor taking into account the contribution of the atoms around the Mn site, inside a sphere with radius 1000 Å. Knowing the eigenvectors of the EFG tensor ($\mathbf{e}_i = (e_{ix}, e_{iy}, e_{iz})$, $i = x, y, z$), which define their principal axes (xyz) with respect to the crystallographic axes (abc), one can calculate the polar angles of the magnetic hyperfine field with respect to the principal axes of the EFG tensor. The calculation revealed that the z-axis and the x-axis are essentially along the long Mn–O bond and b-axis, respectively. At $T = 4.2$ K the pristine stoichiometric $LaMnO_3$ compound follows the so-called A-magnetic structure [1] where the Mn-spins are ferromagnetically coupled within the ac-plane. The successive layers are antiferromagnetically coupled. The magnetic moments of the Mn-spins are parallel with the a-axis ($Pnma$ notation). Since $\hat{\mathbf{m}}(Mn^{3+}) = (1, 0, 0)$ the theoretically calculated angles between the hyperfine magnetic field $\mathbf{H} \parallel \hat{\mathbf{m}}(Mn^{3+})$ with the z-and x-axes of the EFG tensor are $\Theta = \arccos(e_{zx}) = 34.14°$, and $\Phi = 180° + \arctan(e_{yx}/e_{xx}) = 254°$. The calculated values for $(1-\gamma)e^2Qq$, η, Θ and Φ are listed in table 1. Using a program based on Kündig calculations [20] we successfully fitted the magnetically split spectra for all temperatures of the R sample. More specifically, the hyperfine parameters deduced from MS at $T = 4.2$ K are $\delta = 0.491(1)$ mm s^{-1}, $H = 449(1)$ kOe, $e^2Qq = 2.34(2)$ mm s^{-1}, $\Theta = 40.6°$, $\Phi = 252(1)°$ and $\eta = 0.45$. At this point we must note that in order to have a lower χ^2 at the final fitting step we left free, during the fitting, angles Θ and Φ. The fitting gave a slightly larger value for Θ and a lower value for Φ in comparison with the estimated ones from point charge calculation. However, small differences of this kind are expected within the point charge approximation.

Figure 3 also shows the temperature variation of the hyperfine magnetic field of the R $LaMnO_3$ sample. The experimental points are reproduced very well using a power law equation, $H = H_0(1 - T/T_c)^{\beta}$, with $H_0 = 450 \pm 5$ kOe, $T_c = 135.7$ K and $\beta = 0.30 \pm 0.01$. Our results are in good agreement with the neutron data of Moussa *et al* [1] where an exponent $\beta = 0.26$ was deduced from the temperature variation of the ordered magnetic moment. The lower value of the exponent in comparison with the 3D Heisenberg Hamiltonian ($\beta = 0.36$) has been attributed [1] to the anisotropy term [21] or to two-dimensional behaviour [22].

We would like to discuss the differences between the R and AP samples. Neutron diffraction data and high-resolution transmission electron microscopy studies suggest equal numbers of vacant La and Mn sites. Since the AP sample is a cation deficient sample a reasonable expectation is that in this sample the orbital ordering (the long bond) does not have a long range order. Both vacant and Mn^{4+} sites contribute to the interruption of the long range order. This situation may produce an orbital liquid state. Based on the hypothesis of the orbital glass-like state, one can ask why the particular compound transformed from a canted antiferromagnet to a ferromagnetic insulator. In the stoichiometric case, due to the orbital ordering, two neighbour Mn^{3+} ions have their e_g orbitals $|3z^2 - r^2\rangle$ and $|3x^2 - r^2\rangle$ nearly perpendicular, giving rise to ferromagnetic superexchange interactions in the ac-plane. On the other hand, along the b-axis the t_{2g} orbitals give antiferromagnetic interactions. The presence of Mn^{4+} or Mn vacancy disturbs the orbital ordering, permitting some Mn ions to have their e_g orbitals along the b-axis. Consequently the non-stoichiometric compound has ferromagnetic interactions along the three axes, resulting in a ferromagnet that is percolative in character. Our MS spectra reveal that the quadrupole splitting of the AP sample is significantly lower than that of the stoichiometric one. This experimental result means either that the arrangement of the Jahn–Teller distorted MnO_6 octahedra is such that they do not create sizeable distortion or that the local distortion is dynamical in character in comparison to the Mössbauer characteristic time. Furthermore, the magnetic susceptibility of the AP sample shows an abrupt reduction at 110 K, a fact implying that we do not have a simple ferromagnet but a ferromagnet where below 110 K both ferromagnetic and antiferromagnetic interactions should be taken into account.

Finally let us comment on the lower value of the magnetic hyperfine field of the R sample in comparison to the AP one. This reduction is related to the orbital ordering via the supertransferred hyperfine field. The contact field (H_{con}) is the vector sum of a local part $\mathbf{H}_{loc}$ and a supertransferred part $\mathbf{H}_{ST}$. $\mathbf{H}_{loc}$ is proportional to the local 3d spin $\mathbf{S}_0$ on the ion ($S = 5/2$ for the case of Fe^{3+}) while $\mathbf{H}_{ST}$ is the resultant contributions from all single-ligand-bridged Mn^{3+} nearest neighbours n, each one being proportional to the electronic spin $\mathbf{S}_n$ on the nearest neighbour cation site. The resulting field is

$$\mathbf{H}_{hf} \approx H_{loc} + H_{ST} = -C(\mathbf{S}_0/S) + \sum_n B_n(\mathbf{S}_n/S) \tag{1}$$

where C and B_n are positive scalar parameters [23]. The B_n parameters are associated with the geometry of coordination and can be expressed as a function of the Fe–O–Fe or Fe–O–Mn bond angle ϕ_n, namely $B_n = H_\pi + (H_\sigma - H_\pi)\cos^2\phi_n$. In this equation the fields $H_{\pi,\sigma}$ arise from overlap distortions of the Fe cation s orbitals caused by the ligand p orbitals having been unpaired by spin transfer via π and σ bonds into unoccupied 3d orbitals on the nearest neighbour cations n. In the case of insulating manganites the differences in H_{hf} is dominated by H_{ST}. By virtue of theoretical calculations [23] it has been deduced that $H_{loc} \approx -450$ kOe in octahedral oxygen coordinated ferric iron and $B_n(\mathbf{S}/S) \approx -20$ kOe. A ferromagnetic (antiferromagnetic) Fe–O–Mn bond produces a positive (negative) supertransferred field respectively. The $LaMn_{0.99}Fe_{0.01}O_3$ displays the so-called A-antiferromagnetic structure with four ferromagnetic and two antiferromagnetic bonds. In order to justify the observed value of $H_{hf}(0) \approx 450$ kOe we have two explanations.

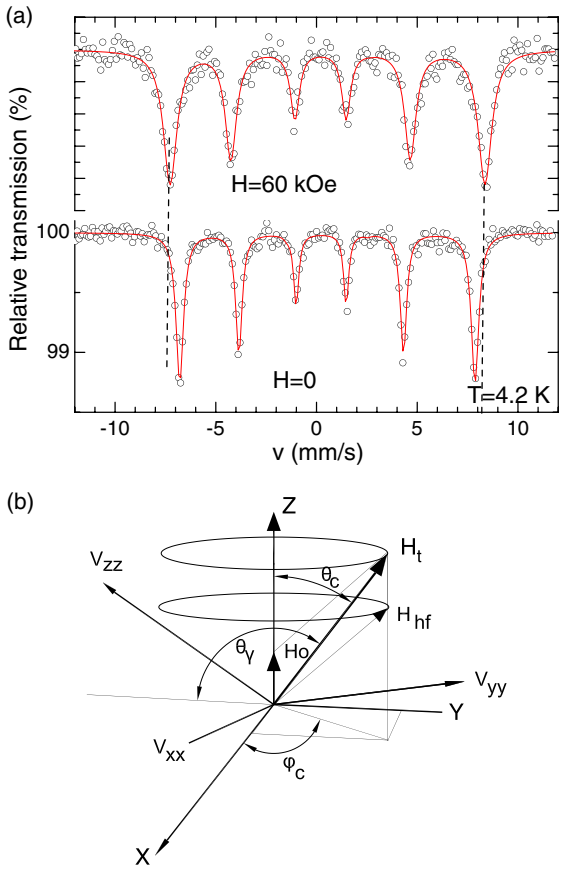

Figure 5. (a) Mössbauer spectra of the R $LaMnO_3$ sample under an external magnetic field at $T = 4.2$ K. The spectrum in zero magnetic field is also included for a direct comparison. (b) Orientation of the hyperfine magnetic field, and of the principal EFG axes of an $LaMnO_3$ crystallite with respect to the laboratory system ($X, Y, Z \parallel H_0$). Since the sample is in powder form the principal axes of the EFG are distributed uniformly in the surface of the unit sphere.

(a) Both $H_{\rm loc}$ and the $B_n(\mathbf{S}_n/S)$ are lower than 450 and 20 kOe respectively.
(b) By speculating that the ferromagnetic contribution of the long ferromagnetic bonds to the $H_{\rm ST}$ is negligible and the remaining two short bonds contribution is cancelled from the two antiferromagnetic bonds along the b-axis, $H_{\rm hf} \approx H_{\rm loc} \approx 450$ kOe.

It should be noted that the hyperfine field at the Mn^{3+} ion determined by specific heat measurements [24] in $LaMnO_3$ is 360 kOe. This value coincides with $H_{\rm hf}$ at the Fe^{3+} ion of the present data by normalizing to the Mn^{3+} spin S, i.e. $H_{\rm hf}(Mn^{3+}) = S(Mn^{3+}) \times H_{\rm hf}(Fe^{3+})/S(Fe^{3+})$.

5. Mössbauer spectra in an external magnetic field

Figure 5(a) shows the Mössbauer spectra of the R sample at $T = 4.2$ K measured under an external magnetic field of 60 kOe. We also include the spectrum for $H = 0$ for a direct comparison. The particular spectrum can not be interpreted on the basis of an antiferromagnet with large or small magnetic anisotropy. In the first case the total hyperfine magnetic field is given by $H_{\rm t} = \sqrt{H_0^2 + H_{\rm hf}^2 + 2H_0H_{\rm hf}\cos\theta}$, where θ is the angle between the external field (H_0) and the hyperfine field. Since we deal with a polycrystalline sample the average magnetic field in the iron site will be $\langle H_{\rm t}\rangle = H_{\rm hf} + (H_0/H_{\rm hf})H_0$. Knowing that $H_{\rm hf} \approx 450$ kOe and $H_0 = 60$ kOe, the expected field is 454 kOe, a value lower than the experimentally observed

481 kOe. Furthermore, broad spectral lines should be expected in this case. In the case of small anisotropy two sextets are expected with $H = H_{\rm hf} \pm H_0$ depending on the antiferro(+) or ferro(−) magnetic coupling of the Fe ion with its Mn neighbours. We could interpret the observed spectra supposing that all the iron spins in the polycrystalline sample are lying on the surface of a cone with its axis along the external field. The geometry of the problem is depicted in figure 5(b). Taking into account our experimental geometry ($\mathbf{k}_\gamma \perp \mathbf{H}_0$) the cone angle will be given by $\arccos(\theta_c) = (H_t^2 - H_0^2 - H_{\rm hf}^2)/(2H_0H_{\rm hf}) = 61^\circ$.

Summarizing, by using Mössbauer spectroscopy we clearly demonstrate that the non-stoichiometric $LaMnO_3$ compound, in comparison to the stoichiometric one, is in a glass orbital state. This glass orbital state does not exhibit cooperative Jahn–Teller distortion on a global and on a local level. The differences of the hyperfine field between stoichiometric and non-stoichiometric $LaMnO_3$ compounds could be explained by taking into account the role of the supertransferred hyperfine field and the kind of the nearest neighbouring magnetic interactions.

Note added. After having finished this paper we became aware of a related work on $La_{0.9}MnO_x$ by M Kopcewicz *et al* 2004 *J. Phys.: Condens. Matter* **16** 4335, where samples with intermediate cation vacancies have been used. In agreement with our results, these authors observed two quadrupole doublets at 300 K. The doublet with large quadrupole splitting comes from iron ions surrounded by six Jahn–Teller Mn^{3+} ions.

References

[1] Moussa F, Hennion M, Rodríguez-Carvajal J, Moudden H, Pinsard L and Revcolevschi A 1996 *Phys. Rev.* B **54** 15149

[2] Skumryev V, Ott F, Coey J M D, Anane A, Renard J-P, Pinsard-Gaudart L and Revcolevschi A 1999 *Eur. Phys. J.* B **11** 401

[3] Tofield B C and Scott W R 1974 *J. Solid State Chem.* **10** 183

[4] van Roosmalen J A M and Cordfunke E H P 1994 *J. Solid State Chem.* **110** 109

[5] Ritter C, Ibarra M R, De Teresa J M, Algarabel P A, Marquina C, Blasco J, García J, Oseroff S and Cheong S-W 1997 *Phys. Rev.* B **56** 8902

[6] Huang Q, Santoro A, Lynn J W, Erwin R W, Borchers J A, Peng J L and Greene R L 1997 *Phys. Rev.* B **55** 14987

[7] Fita I M, Szymczak R, Baran M, Markovich V, Puzniak R, Wisniewski A, Shiryaev S V, Varyukhin V N and Szymczak H 2003 *Phys. Rev.* B **68** 014436
Markovich V, Rozenberg E, Gorodetsky G, Greenblatt M and McCarroll W H 2001 *Phys. Rev.* B **63** 054423

[8] Pissas M, Kallias G, Devlin E, Simopoulos A and Niarchos D 1997 *J. Appl. Phys.* **81** 8

[9] Ogale S B, Shreekala R, Bathe R, Date S K, Patil S I, Hannoyer B, Petit F and Marest G 1998 *Phys. Rev.* B **57** 7841
Hannoyer B, Marest G, Greneche J M, Bathe R, Patil S I and Ogale S B 2000 *Phys. Rev.* B **61** 9613

[10] Tkachuk A, Rogacki K, Brown D E, Dabrowski B, Fedro A J, Kimball C W, Pyles B, Xiong X, Rosenmann D and Dunlap B D 1998 *Phys. Rev.* B **57** 8509

[11] Simopoulos A, Kallias G, Devlin E, Panagiotopoulos I and Pissas M 1998 *J. Magn. Magn. Mater.* **177–181** 860

[12] Chechersky V, Nath A, Isaac I, Franck J P, Ghosh K, Ju H and Greene R L 1999 *Phys. Rev.* B **59** 497
Chechersky V, Nath A, Isaac I, Franck J P, Ghosh K and Greene R L 1999 *J. Phys.: Condens. Matter* **11** 8921

[13] Simopoulos A, Pissas M, Kallias G, Devlin E, Moutis N, Panagiotopoulos I, Niarchos D, Christides C and Sonntag R 1999 *Phys. Rev.* B **59** 1263

[14] Kallias G, Pissas M, Devlin E, Simopoulos A and Niarchos D 1999 *Phys. Rev.* B **59** 1273

[15] Kallias G, Pissas M, Devlin E and Simopoulos A 2001 *Phys. Rev.* B **65** 144426

[16] Simopoulos A, Kallias G, Devlin E and Pissas M 2001 *Phys. Rev.* B **63** 054403

[17] Pissas M and Papavassiliou G 2004 *J. Phys.: Condens. Matter* **16** 6527

[18] Dzialoshinskii I E 1957 *JETP* **5** 1259

[19] Borovik-Romanov A S and Ozhogin V I 1961 *JETP* **12** 18

[20] Kündig W 1967 *Nucl. Instrum. Methods* **48** 219

[21] Pfeuty P, Jasnow D and Fisher M E 1974 *Phys. Rev.* B **10** 2089

[22] Hirota K, Kaneko N, Nishizawa A and Endoh Y 1996 *J. Phys. Soc. Japan* **65** 3736

[23] Sawatzky G A and Van der Woude F 1974 *J. Physique Coll.* **12** C6 47

[24] Woodfield B F *et al* 1997 *Phys. Rev. Lett.* **78** 329